Exciton emission in PTCDA thin films under uniaxial pressure

V. R. Gangilenka, A. DeSilva, and H. P. Wagner
Department of Physics, University of Cincinnati, Cincinnati, Ohio 45221-0011, USA

R. E. Tallman and B. A. Weinstein
Department of Physics, SUNY at Buffalo, New York 14260-1500, USA

R. Scholz
Walter Schottky Institute, Technical University of Munich, 80333 München, Germany
(Received 15 November 2007; revised manuscript received 31 January 2008; published 17 March 2008)

We study the strain dependent photoluminescence (PL) of a 90-nm-thick polycrystalline 3,4,9,10-perylene tetracarboxylic dianhydride film on Si(001) between 20 and 300 K. Uniaxial pressure up to ~5 kbar is applied along the molecular stacking direction using a specially designed pressure cell. With increasing pressure, we find a quenching of the integrated PL intensity, which is mainly attributed to the creation of defects. At low temperature, the charge transfer exciton emission (CT2) gains intensity relative to the Frenkel exciton emission. Furthermore, the CT2 transition reveals a shift to lower energies by up to 24 meV. At room temperature, the PL is dominated by the excimer transition, which also shows a redshift of ~24 meV at the highest uniaxial pressure. The relative increase of the CT2 transition at low temperature and the redshift of the emission bands are attributed to an increased exciton trapping probability and an enhanced binding energy with reduced distance between stacked molecules. This explanation is supported by a comparison with total energy calculations for pairs of adjacent molecules. Moreover, the calculated pressure-induced energy shifts of the CT2 and excimer transitions are in good agreement with the experimentally observed values.

DOI: 10.1103/PhysRevB.77.115206 PACS number(s): 78.55.Kz, 78.20.Bh, 71.35.Aa

I. INTRODUCTION

Recently, molecular thin films have gained significant importance because of their potential for optoelectronic applications, e.g., organic light-emitting diodes (OLEDs),[1–4] inexpensive large-area solar cells,[5,6] and field effect transistors.[7] To date, these applications do not make use of the influence of strain on the electronic and optical properties. Strain effects in "soft" organic materials are much larger (often by a factor of 10) compared to common inorganic solids and, hence, have a great potential to impact novel pressure-sensitive devices, e.g., strain-dependent OLEDs, and organic piezo-optic switches. Despite active research on the optical and electronic properties of organic materials, however, the effects of strain and the related microscopic mechanisms are in many cases not well investigated or understood. Only a few studies report on the pressure dependence of fluorescence spectra in crystalline anthracene,[8,9] polyfluorene,[10–12] poly(*para*-phenylene), and *para*-hexaphenyle.[11] Very few strain-dependent optical investigations have been performed on 3,4,9,10-perylene tetracarboxylic dianhydride (PTCDA) single crystals,[13,14] and on crystalline PTCDA layers.[15]

Thin layers of PTCDA molecules are an ideal molecular system to perform strain-dependent studies. PTCDA molecules form polycrystalline films in the monoclinic space group C_{2h}, with two nearly coplanar molecules in the unit cell.[16,17] Two different crystalline modifications, the α and β phases, are known.[18,19] In both modifications, the planar molecules form stacks along the $\boldsymbol{a}$ direction, which is slightly tilted with respect to the ⟨102⟩ growth direction. The molecules align parallel to the (102) lattice plane, which is equal to the substrate surface.[16] The distance between consecutive molecular planes is shorter than in nonpolar molecular solids such as graphite, which results in a large overlap of molecular π orbitals. The stacking distance can be further reduced by applying uniaxial strain along the soft ⟨102⟩ direction, producing significant modifications of the optical properties.

The excitonic transitions in PTCDA films have been studied intensively using absorption,[20–22] photoluminescence (PL),[15,16,23–25] electroabsorption,[26,27] photoconduction measurements,[28,29] and electron energy loss spectroscopy (EELS).[30] Several theoretical models that include Frenkel excitons, charge transfer (CT) states, and self-trapped excitons[31–40] have been developed to describe the experimental observations. Formally, neutral molecular excitations and CT states interfere via the transfer of an electron or a hole between two adjacent molecules.[34,36] The largest transfer occurs along the stacking direction, remaining, however, rather small: The highest occupied molecular orbital dispersion of about 0.2 eV as obtained from photoemission is compatible with a hole transfer parameter of t_h=0.05 eV.[41] Dimer calculations based on density functional theory and Hartree–Fock reproduce a hole transfer in this range, and the matrix element for electron transfer turns out to be even smaller.[40] The energy of the CT state involving two stacked molecules is ~0.2 eV lower than the energy of a neutral molecular excitation.[40] Therefore, the Frenkel-CT state mixing via fermionic transfer parameters is too small to result in a considerable interference between the respective spectroscopic signatures. Instead, Frenkel excitons are governed by the rather large dipole-dipole interaction between the transition dipoles on adjacent sites,[36–38] resulting in an exciton dispersion with a maximum for small wave vectors and a minimum at the surface of the Brillouin zone,[38,42,43] remaining entirely above the lowest CT states.

 ©2008 The American Physical Society

The first clear indication for such exciton dispersion in crystalline PTCDA was obtained from the wave vector dependence of EELS.[30] However, the observed loss spectra were transformed into a **k**-dependent dielectric function without considering the details of its anisotropy, which has led to an overestimate of the Frenkel-CT state interference. Recent calculations using a pure Frenkel exciton model, which includes the anisotropy and the wave vector dependence of the loss function, have demonstrated that the observed peculiarities of the EELS line shapes can be reproduced quantitatively without any admixture of CT states.[44] Consequently, the excitonic dispersion from EELS[30] and pure Frenkel exciton model calculations[42] are attuned, and the dominating PL mechanism at low temperatures can be understood as a phonon-assisted recombination arising from the minimum of the lowest dispersion branch at the surface of the Brillouin zone.[23,24,37,43]

The weak Frenkel-CT state mixing in PTCDA is more of an exceptional case as demonstrated by the large variety of Frenkel-CT state interference patterns that occur in other perylene compounds.[45] However, the PTCDA with nearly decoupled Frenkel and CT states is an ideal organic material to study the excitonic emission under pressure. Also the theoretical framework, as described above, is an ideal prerequisite to include strain into existing models and to explain the effects of strain on the electronic transitions and on the optical properties in a quantitative way. In this paper, we study the influence of strain on the photoluminescence spectrum of a PTCDA thin film, applying uniaxial pressure along the molecular stacking direction in the temperature range between 20 and 300 K. The experimental results are compared with recent total energy calculations.[40]

II. EXPERIMENTAL DETAILS

The polycrystalline PTCDA films were grown by organic molecular beam deposition (OMBD) at room temperature. Chemically clean *n*-type (001) oriented Si wafers were used as substrates. The Si substrates were cleaned successively in acetone, methanol, and ultrapure water using an ultrasonic bath. Immediately after cleaning, the substrates were transferred into the high vacuum OMBD chamber with a base pressure of 10^{-8} mbar. The PTCDA source material was purified by sublimation under high vacuum (10^{-6} mbar) at 300 °C before being loaded into the Knudsen cell. The PTCDA films were deposited on the Si substrate at room temperature. The deposition rate of 0.01 nm/s at the growth temperature of 320 °C was determined by a calibrated quartz crystal thickness monitor.[15]

A uniaxial pressure cell was used to perform strain-dependent PL measurements ranging from atmospheric pressure to ~5 kbar. Using a screw-driven steel piston within a steel cylinder, the PTCDA film was pressed along the soft ⟨102⟩ direction against a sapphire window. The applied pressures (P_n) were estimated from a comparison with earlier PL measurements on a PTCDA single crystal that were performed in a ruby-calibrated diamond-anvil cell,[14] as described in Sec. III A.

The PTCDA film was photoexcited with a cw laser at 3.05 eV (λ=407 nm) and a power of ~1 mW. The PL spectra were analyzed using a grating monochromator and a GaAs photomultiplier. For variable temperature measurements between 20 and 300 K, the pressure cell with a clamped applied load was placed inside a closed-cycle He cryostat. After having performed temperature-dependent PL measurements at a given pressure, the cryostat was opened, the pressure in the cell was increased, and temperature-dependent PL measurements were again recorded. Care was taken that the optical adjustment as well as the focus size on the sample were not changed during the stepwise increase of the pressure. After finishing the entire measurement series, the pressure in the cell was released and temperature-dependent PL measurements were performed again in order to study the reversibility of the strain effects on the PTCDA film.

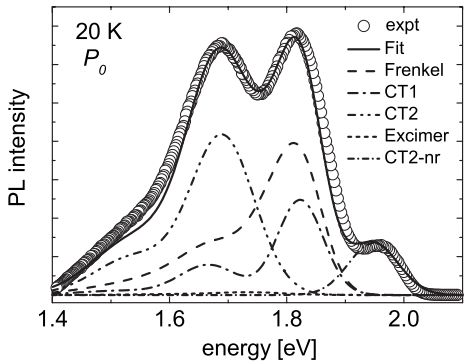

FIG. 1. PL spectra at ambient pressure of a 90-nm-thick PTCDA film on Si(001) excited at 3.05 eV at 20 K. The experimental spectrum (open circles) and different emission channels according to model calculations (lines as labeled) are shown. The resulting calculated spectrum is given as a thick solid line.

III. EXPERIMENTAL RESULTS

A. Photoluminescence spectra at low temperature

Figure 1 shows the PL spectrum of a 90-nm-thick PTCDA film at atmospheric pressure P_0 recorded at 20 K (open circles) as well as various excitonic recombination channels that are reconstructed by model calculations. A detailed description of the line shape analysis used in the present work is given elsewhere.[15,23,24] The strongest band with a peak energy of 1.81 eV is identified as an indirect Frenkel exciton, while the band at 1.82 eV is assigned to a relaxed charge transfer exciton (CT1) between two inequivalent basis molecules within the same unit cell. The PL band with an intensity maximum at 1.68 eV is attributed to a charge transfer exciton (CT2) between two equivalent stacked molecules from adjacent unit cells along the ⟨102⟩ growth direction. In addition, Fig. 1 shows a nonrelaxed charge transfer exciton (CT2-nr) emission at 1.95 eV and a weak excimer band that becomes the dominant emission line at room temperature. All line shapes rely on the same parameters used in previous investigations,[15] except for the CT2 transition energies. The underlying transition between stacked molecules is most sensitive to internal strain,[15,25] depending on the film preparation and thickness. Therefore, in order to better match the present

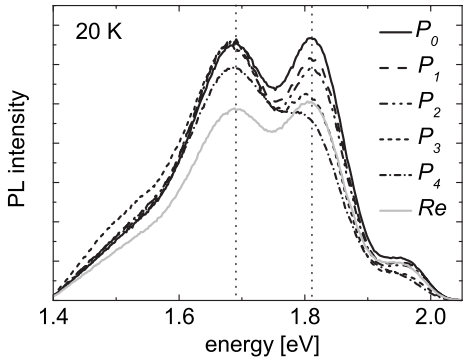

FIG. 2. Uniaxial pressure-dependent PL spectra of a 90-nm-thick PTCDA film on Si(001) excited at 3.05 eV and obtained at 20 K. The applied uniaxial pressure increases from P_0 to P_4. The gray solid line (*Re*) shows the PL spectrum after the strain was released.

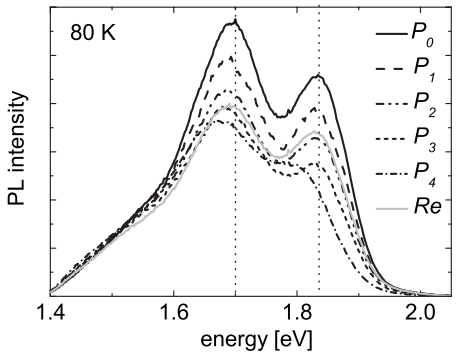

FIG. 4. Uniaxial pressure-dependent PL spectra of a 90-nm-thick PTCDA film on Si(001) excited at 3.05 eV and obtained at 80 K. The applied uniaxial pressure increases from P_0 to P_4. The gray solid line (*Re*) shows the PL spectrum after the strain was released.

thin film sample, the CT2 subband positions have been slightly adjusted to 1.684 and 1.530 eV at ambient pressure.

The pressure-dependent PL spectra of the 90-nm-thick PTCDA film at temperatures 20, 40, and 80 K are displayed in Figs. 2–4. At all temperatures, we find a quenching of the total integrated PL intensity (up to 40%) with increasing pressure. We attribute the reduction of the PL intensity partly to the creation of defects using our pressure cell. Furthermore, the surface roughness of the sapphire window causes strain inhomogeneities within the PTCDA film, which result in a broadening of the PL spectrum and a quenching of the PL intensity. However, at 20 K (see Fig. 2), the intensity of the CT2 band remains almost constant with increasing pressure, while the Frenkel exciton emission is quenched by ~30%. In addition, the CT2 transition exhibits a shift to lower energies by ~10 meV. Up to pressure P_3, the peak positions of the Frenkel exciton and the CT1 transition show only weak strain dependence (again to lower energy); however, this dependence increases at the highest pressure P_4.

Figure 3 shows the pressure-dependent PTCDA emission at 40 K. At this temperature, the strength of the CT2 emission has increased due to a more efficient formation of the corresponding self-trapped exciton state.[15,24] Accordingly,

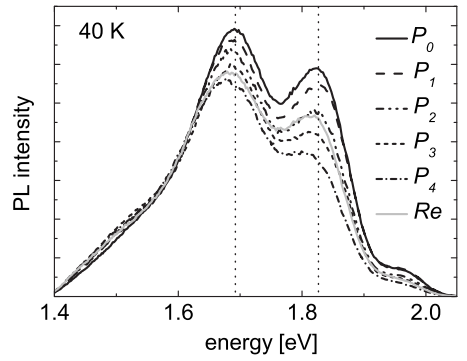

FIG. 3. Uniaxial pressure-dependent PL spectra of a 90-nm-thick PTCDA film on Si(001) excited at 3.05 eV and obtained at 40 K. The applied uniaxial pressure increases from P_0 to P_4. The gray solid line (*Re*) shows the PL spectrum after the strain was released.

the CT2 transition becomes the dominant emission channel at atmospheric pressure P_0. Again, there is an overall reduction of the PL intensity with increasing strain, but the CT2 emission is less affected (~20%) than the Frenkel exciton emission, which shows a 40% reduction at the highest applied pressure (P_4). The CT2 emission is redshifted by ~19 meV at this pressure.

Since the Frenkel exciton emission is significantly reduced at 80 K, the high energy band is predominantly attributed to the CT1 transition[15,24] at this temperature. With increasing pressure, both CT bands exhibit a reduction (~40%) of their emission intensities (see Fig. 4). Again, the peak energy of the CT2 transition shows a significant strain dependence with increasing pressure, revealing a clearly resolved redshift of ~24 meV at the highest applied pressure (P_4), while the pressure dependence of the CT1 transition remains weak up to pressure P_3.

The gray solid lines in Figs. 2–4 show the PL spectra after the strain was released. At all temperatures, the transitions shift back to their original positions and the relative intensity ratio between the CT2 and the Frenkel or CT1 emissions recovers almost completely. However, the total integrated PL intensity is significantly decreased (down to 70% at 80 K) compared with the initial PL spectra taken at atmospheric pressure before applying any strain. This is mainly attributed to some lattice damage inside the film during the pressure measurements. It should be noted, however, that measurements up to ~3 kbar at 80 K led to an 85% recovery of the PL intensity, indicating that most of the strain effects are reversible below a critical strain value.

In order to obtain the energy shift of the CT2 emission as a function of the applied pressure more precisely, all PL spectra at different pressures and temperatures were analyzed using the model line shapes discussed earlier for the PL spectrum at ambient pressure and 20 K (Ref. 15) (see Fig. 1). For these calculations, the full width at half maximum, the areas of the Gaussian functions, and the energy blueshift values given in Table I of Ref. 15 were kept constant. With increasing pressure, the energy positions of the Gaussian subbands of the various emission channels were varied until optimum agreement between the experimental and calculated spectra

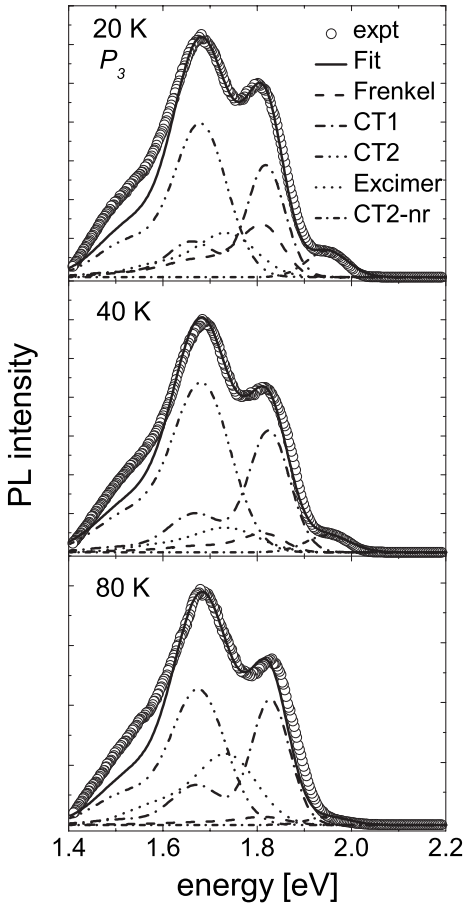

FIG. 5. PL spectra of a 90-nm-thick PTCDA film on Si(001) excited at 3.05 eV at 20, 40, and 60 K at an applied uniaxial pressure P_3. The experimental spectrum (open circles) and different emission channels according to model calculations (lines as labeled) are shown. The resulting calculated spectrum is given as a thick solid line.

was achieved. As expected, the CT2 transition is most sensitive to the applied uniaxial strain in the (102) direction, while according to this fitting procedure, the Gaussians describing the CT1, CT2-nr, and Frenkel excitons exhibit redshifts that are about four times smaller for pressures up to P_3. As an example, Fig. 5 shows the results of the line shape analysis at the applied pressure (P_3) for 20, 40, and 80 K, revealing strongly modified relative intensities of the various PL channels. Deviations of the experimental data from the model fit, in particular, on the low energy side, are attributed to broadening effects that have not been considered in the calculations.

Figure 6 shows the energy position of the zeroth vibronic subband of the CT2 emission, as obtained from the above line shape analysis. As already mentioned, the applied uniaxial pressures P_1-P_4 were estimated from the observed dependence of the CT2 energy on hydrostatic pressure $E(p)=E_0+bp$, with $b=-(4.5\pm0.3)\times10^{-3}$ eV/kbar being the linear pressure coefficient of the PL energy obtained from measurements at 11 K on a PTCDA single crystal. These experiments were performed in a ruby-calibrated diamond-anvil cell with alcohol as a pressure medium.[14] In this esti-

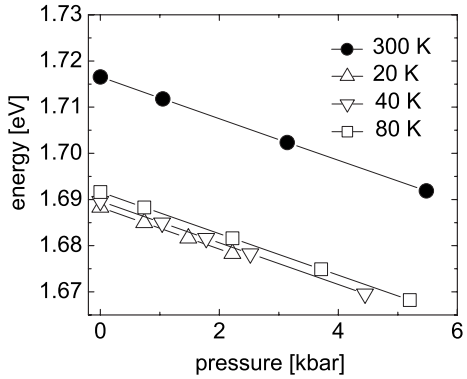

FIG. 6. Energies of the CT2 transition (zeroth vibronic subband) at 20, 40, and 80 K as a function of the estimated applied uniaxial pressure. The CT2 energies were obtained from model calculations fitted to the data as described in the text. Also shown are observed excimer transition energies at 300 K as a function of the estimated uniaxial pressure.

mate of the uniaxial pressure, we assume that the energy shift of the CT2 emission is mainly caused by the compression along the soft ⟨102⟩ direction, while shifts arising from compression (in a hydrostatic cell) or from dilatation (in our uniaxial experiments) within the stiff (102) plane are neglected. We also neglect the tilt of the ⟨102⟩ stacking direction with respect to the substrate normal and the possibility of a pressure-induced modification of the 11° tilt between the molecular normal and the substrate normal. Moreover, we assume that the pressure coefficient b does not vary with temperature, which is usually a higher-order effect.

B. Photoluminescence spectra at room temperature

The predominant emission channel in PTCDA thin films at a temperature higher than 200 K is the excimer transition.[15,24] Figure 7 shows pressure-dependent PL spectra of the PTCDA film at 300 K. With respect to the CT2 transition and the other low-temperature PL features, the excimer PL at atmospheric pressure is significantly broader, revealing a peak energy at 1.716 eV. Similar to the low-

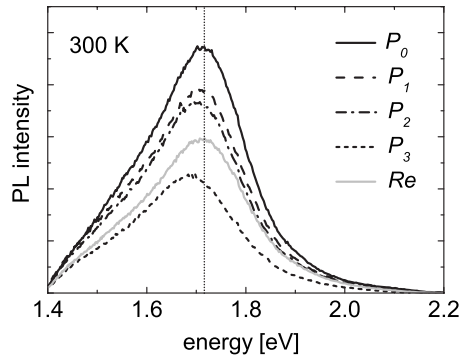

FIG. 7. Uniaxial pressure-dependent PL spectra of a 90-nm-thick PTCDA film on Si(001) excited at 3.05 eV and obtained at 300 K. The applied uniaxial pressure increases from P_0 to P_3. The gray solid line (Re) shows the PL spectrum after the strain was released.

temperature experiments, the integrated PL intensity of the excimer transition decreases with increasing uniaxial pressure. When the applied pressure reaches ~5.4 kbar (P_3), the PL intensity is about a factor of 0.5 lower than at atmospheric pressure. At the largest applied pressure (P_3), the peak energy is 1.691 eV, which corresponds to a ~24 meV shift to lower energy compared to the peak maximum at atmospheric pressure. Since the excimer and CT2 transitions result from recombination across a similar geometry of stacked molecules,[40] we expect similar pressure-dependent shifts of their peak energies. Accordingly, we have estimated the applied uniaxial pressure with the same PL pressure coefficient b. The extracted emission energies as a function of the estimated pressure values are plotted in Fig. 6.

In analogy to the low-temperature measurements, we have recorded the PL spectra at room temperature after the pressure was released to atmospheric pressure. In Fig. 7, the emission spectrum is shown as a gray solid line. The PL maximum returns to the same position as in the original PL spectrum before applying uniaxial pressure. We observe a 65% recovery of the integrated PL intensity. Again, the decrease of PL is attributed to a partial damage of the PTCDA lattice during the application of strain, but the extent of recovery indicates the reversibility of strain effects and, hence, the potential for pressure-sensitive device applications at room temperature.

IV. COMPARISON OF THE STRAIN DEPENDENCE WITH MODEL CALCULATIONS

The relative enhancement of the CT2 emission compared to the other transitions at low temperature is qualitatively attributed to increases in the exciton trapping probability due to the pressure-induced reduction in the intermolecular distance along the (102) direction. In addition, both the CT2 and the excimer PL bands show a large redshift under uniaxial pressure. As the CT2 transition was assigned earlier to the recombination between a negatively charged anionic molecule and a positively charged cationic molecule in a stacked geometry,[40,46] the redshift at increased pressure can directly be related to a lowering of the CT transition energy at a reduced stacking distance. Due to the fact that the CT state resembles a nanoscopic parallel plate capacitor, this dependence on the stacking distance is intuitively expected, and from previous calculations of the CT transition as a function of stacking distance, the slope of the CT energy with respect to the length $a=|\boldsymbol{a}|$ of the stacking vector $\boldsymbol{a}$ was found to be about $dE(\mathrm{CT2})/da \sim 0.5$ eV/Å.[40] The excimer PL, on the other hand, was assigned to a dipolar CT transition in a deformed molecular dimer conserving inversion symmetry, so that the two molecules in this self-trapped excitonic state are both neutral. The transition dipoles of the two possible directions of the CT transitions interfere constructively, speeding up the radiative recombination time by a factor of about 2 with respect to PL from the CT2 state.[24] The slope of the excimer energy with respect to the length of the stacking vector $\boldsymbol{a}$ has been calculated to be close to the value for the CT2 state.[40]

In order to quantify the redshift of the CT2 and excimer PL bands, it is crucial to determine the element of the compliance tensor along the soft $\boldsymbol{a}$ axis. The compliance tensor relates the applied stress to a macroscopic strain, which, in turn, corresponds to length and/or angular changes within the unit cell. Accordingly, we have investigated the pressure-dependent changes of a single PTCDA crystal under hydrostatic pressure in a diamond-anvil cell by microphotography. The compressibility parallel to the $\boldsymbol{a}$ lattice vector, corresponding to the long axis of the crystallite, was determined directly by comparing the crystal length at high pressure to the initial length at atmospheric pressure. Photographic images at 1 and 55 kbar (300 K) are shown in Fig. 8, where the pressure-induced compression parallel to the $\boldsymbol{a}$ axis of the crystal is clearly seen. The observed length scaling $L(p)/L_0$ in this direction measures the relative change of the lattice constant $a(p)/a_0$ that is plotted against hydrostatic pressure p in Fig. 9.

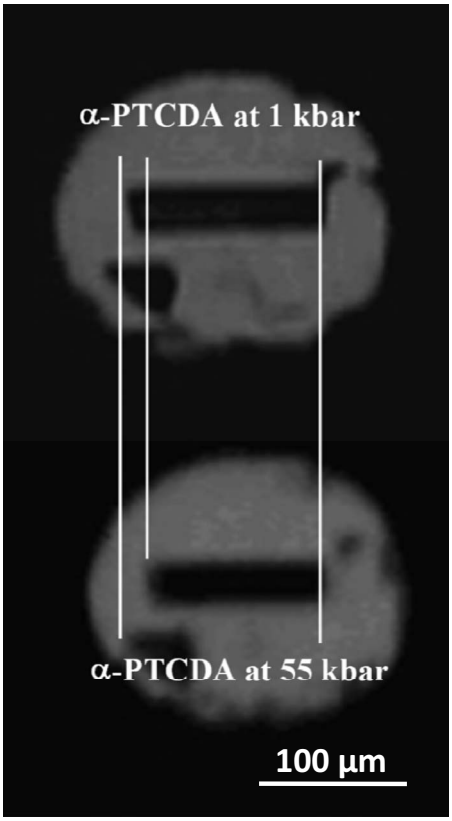

FIG. 8. Photos under identical optical conditions showing the $\boldsymbol{a}$-axis length change of an α-PTCDA crystal between 1 and 55 kbar hydrostatic pressure in a diamond-anvil cell at 300 K.

Assuming that the intermolecular potential along the stacking direction $\boldsymbol{a}$ can be described by a Morse potential close to the equilibrium lattice constant $a_0=3.72$ Å, we use the following parametrization:

$$V(x) = V_0(e^{-2\lambda x} - 2e^{-\lambda x}) + \text{const}, \tag{1}$$

where $x=a-a_0$ is the change of the lattice constant. The formula for the slope dV/dx can easily be inverted, resulting in the following dependence of the lattice constant on pressure p:

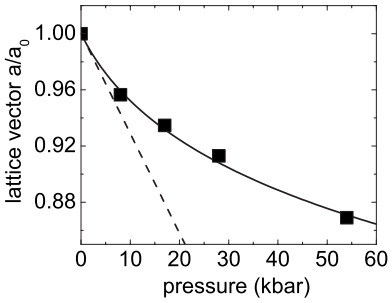

FIG. 9. Length scaling of the PTCDA crystal parallel to the ***a*** axis as a function of pressure. The solid line shows the best fit using Eq. (6) and the dashed line gives the linear pressure dependence of $a(p)/a_0$ according to Eq. (4).

$$\lambda x = -\ln\left[\left(1+\sqrt{1+\frac{2pA}{\lambda V_0}}\right)\Big/\,2\right], \tag{2}$$

where $A=119$ Å^2 is the area per molecule, calculated from half of the size of the unit cell $bc'=11.96\times19.89$ Å^2 in the (102) plane parallel to the substrate. The linear compressibility along that direction is given by

$$\beta_a = \frac{A}{2\lambda^2 V_0 a_0} \tag{3}$$

and the lattice constant varies as

$$a(p)/a_0 = 1-\beta_a p \tag{4}$$

to leading order. By inserting Eq. (3) into Eq. (2), the dependence of the lattice constant can be expressed as follows:

$$\lambda x = -\ln\left\{\frac{1+\sqrt{1+4p\lambda a_0\beta_a}}{2}\right\} \tag{5}$$

so that the normalized lattice constant is given by

$$\frac{a(p)}{a_0} = 1-\frac{1}{a_0\lambda}\ln\left(\frac{1+\sqrt{1+4(\lambda a_0)\beta_a p}}{2}\right). \tag{6}$$

In Fig. 9, the full solid shows a fit according to Eq. (6), with the parameters $\lambda a_0=5.52$ and $\beta_a=(7.1\pm0.7)\times10^{-3}$ kbar^{-1}, and the dashed line gives the linear approximation according to Eq. (4). The excellent agreement of the Morse potential with the observed nonlinear pressure dependence of the lattice constant indicates that the nonparabolic shape of the intermolecular potential is of utmost importance for a quantitative assignment of the geometric response to an applied uniaxial pressure.

Total energy calculations for pairs of adjacent molecules also allow an estimate of the compressibility for a one-dimensional reduction in the stacking distance of PTCDA molecules along the ⟨102⟩ direction. From a van der Waals potential along the stacking direction estimated from dimer calculations in second-order Møller–Plesset perturbation theory (MP2), the region around the equilibrium lattice constant can again be parametrized with a Morse potential. In such a construction based on a MP2 correlation energy obtained with the 3-21G variational basis set,[40] one finds $\lambda a_0=5.63$ and a compliance constant $\beta_a=7.3\times10^{-3}$ kbar^{-1}, in excellent agreement with the fit to the observed compression of the lattice constant a. It should be mentioned, however, that a similar construction applied to MP2 calculations in the larger variational sets SVP and TZVP[47] gives a smaller compressibility $\beta_a=6.1\times10^{-3}$ kbar^{-1}, still in reasonable agreement with the experimental observations.

Having determined the response of the lattice constant to the uniaxial pressure from Eq. (2), we can make theoretical estimates of the redshift of the CT2 and excimer transitions. Under pressure, the intermolecular potential in the electronic ground state, the excimer state, and the pair of oppositely charged ionized molecules (CT2) is given by the sum of the respective potential surface at zero pressure and a linear term proportional to the applied pressure. Within the pressure range reported in Fig. 6, each excited potential can still be fitted to a nonparabolic Morse potential so that the position of the minimum can be obtained from the parameters of the fit. For the potential energy surfaces of the excimer and the CT2 state, this procedure results in a shift of the potential minimum by about −0.066 Å at $p=5$ kbar.

From the dependence of the CT2 and excimer transition energies on stacking distance, we can estimate a redshift of 31 meV for the PL from the CT2 state, and of 33 meV for the excimer PL. As an average over the pressure interval from zero pressure to 5 kbar, this corresponds to pressure coefficients of the transition energies of $b=-6.2$ meV/kbar for CT2, and of $b=-6.6$ meV/kbar for the excimer.

Both theoretical estimates are in the same range as the pressure coefficient of $b=-4.5$ meV/kbar determined by isotropic pressure,[14] which has been applied to calibrate the slopes in Fig. 6. Moreover, the smaller compliance constant of $\beta_a=6.1\times10^{-3}$ kbar^{-1} deduced from better converged MP2 calculations[47] would result in more rigid potential energy surfaces of the CT2 and excimer states. In turn, this increased rigidity reduces the pressure dependence of the transition energies by about one-sixth, bringing them somewhat closer to the experimental value of $b=-4.5$ meV/kbar determined for the CT2 state in bulk crystals.[14] The remaining deviation of the calculated values from experiment may be due to the neglect of pressure-induced changes in the ***b*** and ***c*** lattice vectors, which cannot be investigated with models based on only two molecules, and from principal shortcomings of the Hartree-Fock- and MP2-based methods used in the calculations.[40,47]

V. SUMMARY

In the present work, we have investigated the pressure dependence of the various emission channels in a 90-nm-thick PTCDA film grown on Si(001). The experiments were performed at 20, 40, 80, and 300 K using a specially designed uniaxial pressure cell. The applied pressure was estimated from PL measurements on a PTCDA single crystal that were performed in a ruby-calibrated diamond-anvil cell under hydrostatic pressure.

At low temperature (20, 40, and 80 K), we observe a strong reduction of the Frenkel exciton, CT1, and CT2-nonrelaxed intensities with increasing pressure, while the

CT2 emission intensity is only slightly affected. In addition, the CT2 transition exhibits a significant redshift with increasing pressure, while the other self-trapped exciton transitions and the Frenkel exciton show a comparatively weak shift to lower energy. At 300 K, the PL is dominated by the excimer emission, which slightly weakens with increasing pressure. The excimer band shows a redshift of ~24 meV at the highest applied pressure of ~5.4 kbar.

The decrease of the integrated PL intensity with increasing pressure is mainly attributed to the generation of defects in the PTCDA film. When the pressure is released, the PL spectrum and the total PL intensity partly recover, indicating that the observed strain effects are reversible to a large extent.

The relative enhancement of the CT2 emission under pressure is attributed to an increased probability to form the corresponding self-trapped exciton state. The redshifts of the CT2 and excimer transition energies are directly related to the reduced intermolecular distance along the $\langle 102 \rangle$ direction. Comparisons with recent model calculations[40] support these qualitative conclusions and provide a linear compressibility of $\beta_a \approx 0.007$ kbar^{-1} together with energy shifts of the CT2 and excimer transitions of around $b=-6$ meV/kbar, in reasonable agreement with the experimentally observed values.

The obtained results illustrate the importance of strain for the optical properties of soft organic layers. They also emphasize the potential of strain for device engineering: In stacked organic materials such as PTCDA, large strain-induced modifications of the emissive properties occur already at moderate applied pressures.

[1] C. W. Tang and S. A. Van Slyke, Appl. Phys. Lett. **51**, 913 (1987).
[2] M. A. Baldo, D. F. O'Brien, Y. You, A. Shoustikov, S. Sibley, M. E. Thompson, and S. R. Forrest, Nature (London) **395**, 151 (1998).
[3] M. A. Baldo, M. E. Thompson, and S. R. Forrest, Nature (London) **403**, 750 (2000).
[4] J. Huang, M. Pfeiffer, A. Werner, J. Blochwitz, S. Liu, and K. Leo, Appl. Phys. Lett. **80**, 139 (2002).
[5] P. Peumans, V. Bulovic, and S. R. Forrest, Appl. Phys. Lett. **76**, 2650 (2000).
[6] D. Meissner and J. Rostalski, Synth. Met. **121**, 1551 (2001).
[7] R. Hajlaoui, G. Horowitz, F. Garnier, A. Arce-Brouchet, K. Laigre, A. El Kassimi, F. Demanze, and K. Kouki, Adv. Mater. (Weinheim, Ger.) **9**, 389 (1997).
[8] Z. A. Dreger, H. Lucas, and Y. M. Gupta, J. Phys. Chem. B **107**, 9268 (2003).
[9] R. Sonnenschein, K. Syassen, and A. Otto, J. Chem. Phys. **74**, 4315 (1981).
[10] C. M. Martin, S. Guha, M. Chandrasekhar, H. R. Chandrasekhar, R. Guentner, P. Scanduicci de Freitas, and U. Scherf, Phys. Rev. B **68**, 115203 (2003).
[11] S. Guha and M. Chandrasekhar, Phys. Status Solidi B **241**, 3318 (2004).
[12] B. Y. Okamoto and H. G. Drickamer, J. Chem. Phys. **61**, 2870 (1974).
[13] A. Jayaraman, M. L. Kaplan, and P. H. Schmidt, J. Chem. Phys. **82**, 1682 (1985).
[14] R. E. Tallman, B. A. Weinstein, A. DeSilva, and H. P. Wagner, Phys. Status Solidi B **241**, 3334 (2004).
[15] H. P. Wagner, A. DeSilva, and T. U. Kampen, Phys. Rev. B **70**, 235201 (2004).
[16] S. R. Forrest, Chem. Rev. (Washington, D.C.) **97**, 1793 (1997).
[17] A. J. Lovinger, S. R. Forrest, M. L. Kaplan, P. H. Schmidt, and T. Venkatesan, J. Appl. Phys. **55**, 476 (1984).
[18] A. J. Lovinger, S. R. Forrest, M. L. Kaplan, P. H. Schmidt, and T. Venkatesan, Bull. Am. Phys. Soc. **28**, 363 (1983).
[19] M. Möbus, N. Karl, and T. Kobayashi, J. Cryst. Growth **116**, 495 (1992).
[20] V. Bulović, P. E. Burrows, S. R. Forrest, J. A. Cronin, and M. E. Thompson, Chem. Phys. **210**, 1 (1996).
[21] F. F. So and S. R. Forrest, Phys. Rev. Lett. **66**, 2649 (1991).
[22] H. P. Wagner, V. R. Gangilenka, A. DeSilva, H. Schmitzer, R. Scholz, and T. U. Kampen, Phys. Rev. B **73**, 125323 (2006).
[23] A. Yu. Kobitski, R. Scholz, I. Vragović, H. P. Wagner, and D. R. T. Zahn, Phys. Rev. B **68**, 155201 (2002).
[24] A. Yu. Kobitski, R. Scholz, D. R. T. Zahn, and H. P. Wagner, Phys. Rev. B **68**, 155201 (2003).
[25] H. P. Wagner, A. DeSilva, V. R. Gangilenka, and T. U. Kampen, J. Appl. Phys. **99**, 024501 (2006).
[26] Z. Shen and S. R. Forrest, Chem. Phys. Lett. **236**, 129 (1995).
[27] E. I. Haskal, Z. Shen, P. E. Burrows, and S. R. Forrest, Phys. Rev. B **51**, 4449 (1995).
[28] N. Karl, A. Bauer, J. Holzäpfel, J. Marktanner, M. Möbus, and F. Stölzle, Mol. Cryst. Liq. Cryst. Sci. Technol., Sect. A **252**, 243 (1994).
[29] V. Bulović and S. R. Forrest, Chem. Phys. Lett. **238**, 88 (1995).
[30] M. Knupfer, T. Schwieger, J. Fink, K. Leo, and M. Hoffmann, Phys. Rev. B **66**, 035208 (2002).
[31] V. M. Agranovich, R. D. Atanasov, and G. F. Bassani, Chem. Phys. Lett. **199**, 621 (1992).
[32] V. Bulović, P. E. Burrows, S. R. Forrest, J. A. Cronin, and M. E. Thompson, Chem. Phys. **210**, 1 (1996).
[33] V. Bulović and S. R. Forrest, Chem. Phys. **210**, 13 (1996).
[34] M. Hoffmann, K. Schmidt, T. Fritz, T. Hasche, V. M. Agranovich, and K. Leo, Chem. Phys. **258**, 73 (2000).
[35] M. H. Hennessy, Z. G. Soos, R. A. Pascal Jr., and A. Girlando, Chem. Phys. **245**, 199 (1999).
[36] M. Hoffmann and Z. G. Soos, Phys. Rev. B **66**, 024305 (2002).
[37] I. Vragović, R. Scholz, and M. Schreiber, Europhys. Lett. **57**, 288 (2002).
[38] I. Vragović and R. Scholz, Phys. Rev. B **68**, 155202 (2003).
[39] R. Scholz and M. Schreiber, J. Lumin. **112**, 303 (2005).
[40] R. Scholz, A. Y. Kobitski, D. R. T. Zahn, and M. Schreiber, Phys. Rev. B **72**, 245208 (2005).
[41] H. Yamane, S. Kera, K. K. Okudaira, D. Yoshimura, K. Seki, and N. Ueno, Phys. Rev. B **68**, 033102 (2003).

[42] R. Scholz, I. Vragović, A. Yu. Kobitski, G. Salvan, T. U. Kampen, M. Schreiber, and D. R. T. Zahn, in *Organic Nanostructures: Science and Applications*, Proceedings of the International School of Physics "Enrico Fermi" Course CXLIX, edited by V. M. Agranovich and G. C. La Rocca (IOS, Amsterdam, 2002), pp. 379–402.

[43] R. Scholz, I. Vragović, A. Yu. Kobitski, M. Schreiber, H. P. Wagner, and D. R. T. Zahn, Phys. Status Solidi B **234**, 402 (2002).

[44] I. Vragović, M. Schreiber, and R. Scholz, J. Lumin. **110**, 284 (2004).

[45] J. Mizuguchi and K. Tojo, J. Phys. Chem. B **106**, 767 (2002).

[46] R. Scholz, A. Yu. Kobitski, I. Vragović, T. U. Kampen, D. R. T. Zahn, and H. P. Wagner, in *Physics of Semiconductors 2002*, edited by A. R. Long and J. H. Davies, IOP Conf. Proc. No. 171 (Institute of Physics, Bristol, 2002), p. 266.

[47] A. Abbasi and R. Scholz (unpublished).